Control of Density Fluctuations and Electron Transport in the Reversed-Field Pinch

N. E. Lanier, D. Craig, J. K. Anderson, T. M. Biewer, B. E. Chapman, D. J. Den Hartog, C. B. Forest, and S. C. Prager
Department of Physics, University of Wisconsin-Madison, Madison, Wisconsin 53706

D. L. Brower and Y. Jiang
Department of Electrical Engineering, University of California at Los Angeles, Los Angeles, California 90095-1594
(Received 24 March 2000)

A recent study conducted on the Madison Symmetric Torus reversed-field pinch has shown that control of density fluctuations can be achieved through modification of the current density profile. Most of the power in the density fluctuations is directly associated with core-resonant resistive tearing modes. We report that, during auxiliary current drive experiments, these density fluctuations are reduced about an order of magnitude over the entire plasma cross section and the resulting electron confinement is increased eightfold.

PACS numbers: 52.25.Fi, 52.25.Gj, 52.55.Ez

The control of particle and energy transport arising from plasma fluctuations continues to be a significant goal of plasma physics—both to understand the link between fluctuations and transport, and for application to fusion energy. In various magnetic configurations, particularly the tokamak, substantial progress has occurred in the reduction of transport arising from fluctuations in the electric field, often referred to as electrostatic turbulence [1,2]. In the reversed-field pinch (RFP) configuration [3], magnetic fluctuations have long been expected to be the dominant source of transport, particularly in the plasma core [4]. The presence of magnetic fluctuations of multiple wavelengths can produce stochasticity in the magnetic field line trajectories. This is consistent with direct measurements of magnetic fluctuation induced particle transport [5] and energy transport [6] in the outer region of RFP plasma.

Recently, it was established experimentally that the modification of the current density profile reduces magnetic fluctuations (measured at the edge) by a factor of 2, and increases global energy confinement time (the energy loss time if the plasma were unheated) fivefold [7]. Measurements of the electron temperature profile in similar improved confinement RFP plasmas established that energy transport was indeed being reduced in the plasma core [8], consistent with the expected link between energy transport and magnetic stochasticity.

In this Letter, we establish experimentally that diffusive transport of electrons is dramatically affected by current profile control, suggesting that particle transport is strongly linked to magnetic stochasticity. The global electron confinement time is increased by a factor of 8, similar to the gains in energy confinement. Moreover, the radial electron flux is significantly reduced over the entire cross section, revealing the strong influence of magnetic fluctuations on the core particle transport. The link between magnetic stochasticity and particle transport likely extrapolates to other plasma configurations that are dominated by magnetic fluctuations (such as the spheromak), as well as astrophysical plasmas embedded in fluctuating magnetic fields. We also establish that the density fluctuations are reduced by a large factor over the entire plasma cross section, and are associated with the tearing fluctuations that are known to dominate the magnetic fluctuations. Prior fluctuation measurements in improved confinement plasmas inferred internal fluctuation behavior from edge measurements.

Four experimental tools enable this study in the Madison Symmetric Torus (MST) [9] reversed-field pinch: a fast multichord far-infrared (FIR) laser interferometer [10,11] to measure both equilibrium and fluctuating electron density behavior throughout the plasma, two multichord arrays for the detection of both H_α (D_α) and soft x-ray radiation to quantitatively constrain the electron source from ionization of neutral hydrogen (deuterium) and low-Z impurities, a 64-position toroidal array of magnetic pickup coils to monitor equilibrium and fluctuating magnetic field information, and inductive current profile control (known as pulsed poloidal current drive, or PPCD) to alter the magnetic fluctuations and particle transport [12].

The radial electron flux (Γ), described in the continuity equation, $dn_e/dt + \nabla \cdot \Gamma = S_H + S_Z$, is obtained by measuring the balance between the changes in total electron content and electron source rate. The multichord FIR interferometer yields electron density information (dn_e/dt), while quantitative measurements from radiation detector arrays constrain the electron source from ionization of neutral hydrogen (S_H) and impurities (S_Z).

The FIR interferometer measures the chord-integrated electron density (I) at eleven impact parameters ranging from $r/a = -0.62 \rightarrow +0.83$, where $I = \int_{-L/2}^{+L/2} n_e(z)\, dz$. Local density profiles are obtained from chord-integrated measurements via the MSTFIT reconstruction code [13], which assumes that electron density is a flux function, and utilizes a least squares fit to determine the coefficients of a set of spline basis functions. Errors in the profile are obtained by inverting various perturbations of the raw data in a Monte Carlo fashion. With a frequency response of 250 kHz, the FIR system is well suited to the detection of the dominant electron density fluctuations in MST.

 0031-9007/00/85(10)/2120(4)$15.00

These fluctuations are large scale and low frequency (<30 kHz). Laser interferometry has been previously employed to study electron density fluctuations [14,15] and their relationship to transport [16–18] in standard discharges in the ZT-40M RFP. We extend this work to include toroidal and poloidal mode number spectra, correlation with magnetic fluctuations, and behavior in improved confinement PPCD discharges.

The electron source profile from neutral hydrogen is measured with a nine-chord array of filtered monochromators that detects H_α emission. For the temperatures of MST plasmas, the ionization rate of neutral hydrogen is proportional to the excitation rate of the $2s$-$3p$ (H_α) transition [19]. The chord-integrated H_α measurements are then inverted to yield local source rates from neutral hydrogen. The symmetric component of the electron source profile is inverted in a similar manner as done for the density. However, additional parameters are incorporated to correctly consider asymmetries in sourcing resulting from the plasma interactions with the limiter.

Impurity sourcing of electrons is dominated by aluminum, carbon, and oxygen. To quantify their contribution, three distinct soft x-ray arrays placed at impact parameters of $r/a = +0.02$, $+0.40$, and $+0.77$ make absolute radiation flux measurements from K shell transitions of AL XII, O VII, O VIII, C V, and C VI. These measurements, along with electron density and temperature information, are used in the multi-ion species transport (MIST) code [20] to constrain impurity fractions. In general, we find impurity sourcing in standard discharges to be negligible. However, during PPCD, when the neutral hydrogen population drops in the core, sourcing from impurities becomes comparable to that of hydrogen and must be considered.

Measurements for this experiment were conducted in both standard and PPCD-induced high confinement discharges. With two notable exceptions, both cases were deuterium fueled and had similar global plasma parameters with peak plasma currents of ~220 kA and discharge lengths near 30 ms. The principal difference is that, for PPCD plasmas, an auxiliary poloidal electric field is initiated, via extraction of toroidal flux, 8 ms after startup. Furthermore, due to the large increase in electron density during PPCD, often as much as 60%, the initial density was lowered, so that at peak confinement the chord-integrated electron density is similar to that in standard plasmas. In standard discharges the density profiles are flat in the core with a steep gradient at the edge (Fig. 1a). The electron source, which is dominated by ionization of neutral deuterium, appears to be quite broad with substantial sourcing deep into the core (Fig. 1b). This leads to a radial electron flux, displayed in Fig. 1c, that ranges from $\sim 2.0 \times 10^{+20}$ m^{-2} s^{-1} in the core rising to $\sim 3.0 \times 10^{+21}$ m^{-2} s^{-1} at the plasma boundary. These edge values are consistent with past probe measurements which reported electrostatic fluctuation induced electron flux in the extreme edge to be $1.5 \rightarrow 5.0 \times 10^{+21}$ m^{-2} s^{-1} [21].

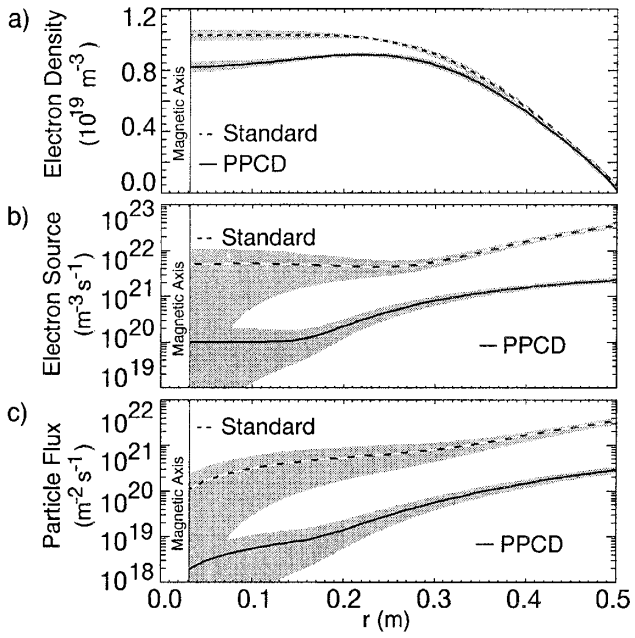

FIG. 1. Radial profiles of (a) electron density, (b) electron source (impurities included), and (c) radial electron flux for standard and PPCD discharges.

During PPCD, the radial electron flux drops more than an order of magnitude, with the core showing the most dramatic reduction (Fig. 1c). With the reduction in plasma wall interaction, wall fueling drops and the resulting electron sourcing from neutral deuterium is greatly diminished. The density profile broadens and becomes hollow (Fig. 1a). This gradient formation in the core is a clear indicator of confinement improvement. The radial electron flux is reduced by almost 2 orders of magnitude in the core, yielding an average flux of $\sim 2.0 \times 10^{+18}$ m^{-2} s^{-1} for $r/a < 0.3$. We calculate the global electron confinement time in these cases to be about ~4.7 ms, whereas in standard cases it is measured to be ~0.6 ms.

Concurrent with the improvements in electron confinement and diminution of magnetic fluctuations during PPCD, a dramatic reduction in the chord-integrated density fluctuations is also observed. Below we first describe density fluctuations in standard plasmas—the amplitude, wave number content, and correlation with the individual spatial Fourier harmonics of the magnetic fluctuations. This identifies the bulk of the density fluctuations as tearing modes—with the exception of those fluctuations in the extreme edge. We then discuss the change in these fluctuations during enhanced confinement PPCD discharges.

It has long been known that the dominant magnetic fluctuations in the RFP are resistive tearing instabilities [22]. For MST, the dominant modes are the $m = 1$, $n = 6 \rightarrow 9$ helical modes (where m and n are poloidal and toroidal mode numbers) [23,24]. The amplitudes of specific modes are obtained from a Fourier decomposition of the data from the 64-position magnetic coil array. Though resonant in the core, the perturbations are global, extending to

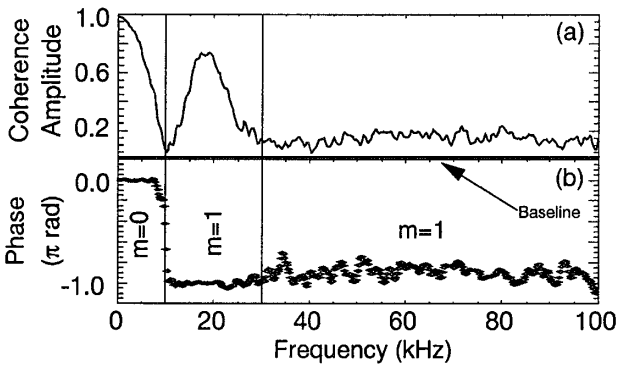

FIG. 2. Coherence amplitude (a) and phase (b) between $r/a = 0.62$ inboard and $r/a = 0.83$ outboard FIR chords. Both chords are at the same toroidal angle.

the plasma edge. Typical fluctuations levels during standard discharges are measured to be about 1% at the plasma boundary. During PPCD, these fluctuations are reduced by a factor of 2.

While magnetic fluctuation amplitudes are of an order of a few percent, local measurements of the density fluctuations in the plasma edge can exceed 50% in some conditions. Inspection of the chord-integrated density fluctuation power spectrum allows the fluctuations to be classified into three categories: ultralow (<10 kHz), low (10 → 30 kHz), and high (>30 kHz) frequencies. The wave number content of these fluctuations is determined from correlations between poloidally and toroidally separated FIR chords. For example, the correlation between inboard and outboard density chords, displayed in Figure 2, shows that the density fluctuations are highly coherent and that those in the ultralow range (<10 kHz) are $m = 0$-like, while the fluctuations above 10 kHz display a clear $m = 1$ nature.

The relationship between the magnetic and density fluctuations is explored by correlating the density information acquired from the FIR interferometer with the Fourier decomposed signals obtained from the toroidal magnetic array. The density fluctuation power that is coherent with the $m = 1$, $n = 5 \rightarrow 15$ core-resonant tearing modes is displayed in Fig. 3 along with the total and incoherent power for impact parameters of $r/a = 0.11$, 0.54, and 0.83. We see that centermost chords are poorly coherent with the $m = 1$ magnetic fluctuations, as would be expected since the central chords are relatively insensitive to $m =$ odd perturbations (Fig. 3a). At larger impact parameters, virtually all of the power between 10 and 20 kHz is coherent with the $n = 5 \rightarrow 15$ tearing mode perturbations (Fig. 3b). In the plasma edge, the contribution from smaller scale, higher frequency, magnetic and electrostatic fluctuations increases (Fig. 3c).

During enhanced confinement PPCD discharges, a dramatic reduction in the chord-integrated density fluctuations is observed (Fig. 4). This quiescence occurs over the entire plasma cross section with all chords showing similar decreases. The density fluctuation power drop is most significant in the tearing mode frequencies (10 → 20 kHz),

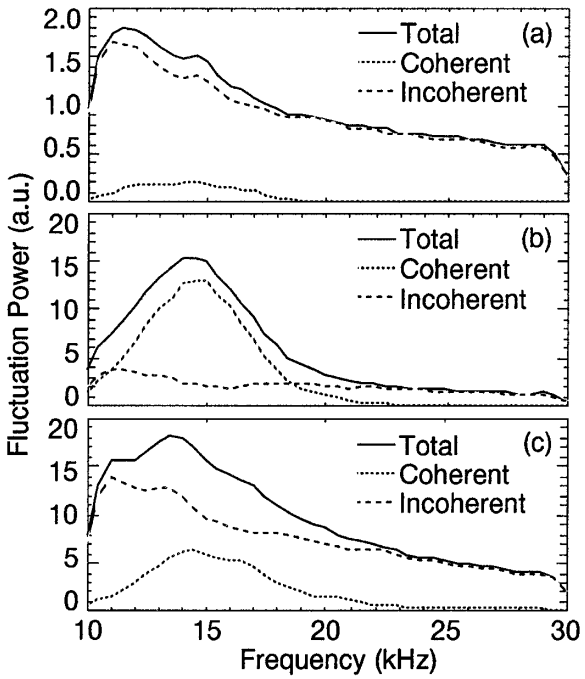

FIG. 3. The total, coherent, and incoherent density fluctuation power for impact parameters of $r/a =$ (a) 0.11, (b) 0.54, and (c) 0.83.

where reductions of fiftyfold have been observed. Although the tearing mode fluctuation amplitudes are diminished during PPCD, the density and magnetic fluctuations become more coherent. This apparent disproportionate reduction in the incoherent fluctuations suggests a decrease in electrostatic fluctuations or possibly magnetic stochasticity, since this stochasticity would serve to decouple the density and magnetic fluctuations.

The density fluctuation radial profiles ($\tilde{n}$) of the core-resonant toroidal harmonics, obtained by inverting the correlated component of the chord-integrated measurements, also show a large reduction during current profile experiments. The profiles for the $n = 6 \rightarrow 9$ harmonics, displayed in Figs. 5a–5d, are broad with amplitudes $\sim 1\% \rightarrow 2\%$ in standard discharges. Moreover, as toroidal mode number (n) increases, the peak in the fluctuation profile moves outward in radius. This is consistent with the expectation that, for a constant density gradient, the density fluctuation from a magnetic tearing mode should peak near its rational surface. During PPCD, $\tilde{n}$ drops by an order of

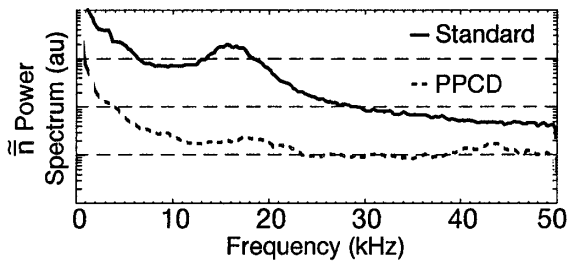

FIG. 4. $\tilde{n}$ frequency spectrum for standard and PPCD discharges, for a chordal impact parameter of $r/a = 0.54$.

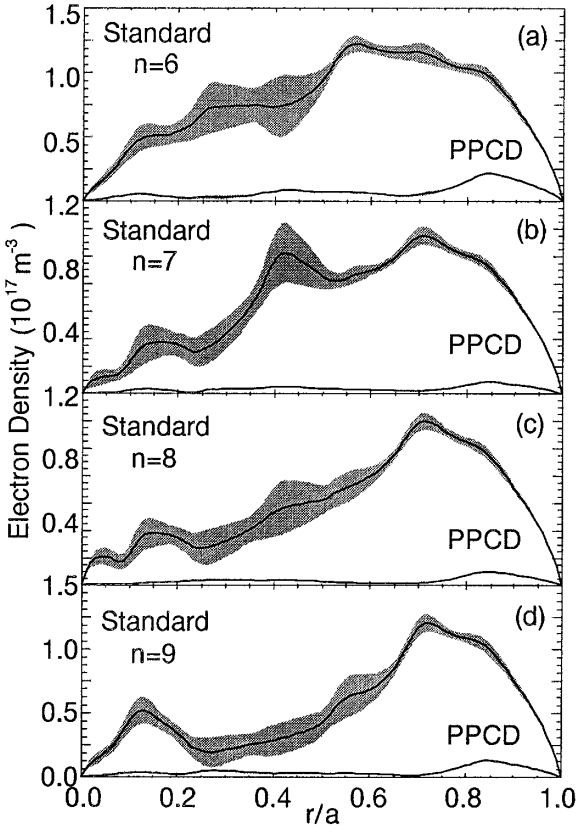

FIG. 5. Radial electron density fluctuation profiles $[\tilde{n}(r)]$, during both standard and PPCD discharges, for the $m = 1$: (a) $n = 6$, (b) $n = 7$, (c) $n = 8$, and (d) $n = 9$ helicities.

magnitude and peaks near the toroidal magnetic field reversal surface. This peaking at the reversal surface is an indication that the very steep density gradient is playing a role in these fluctuations.

In summary, we have shown that electron confinement can be improved greatly—by a factor of 8—in RFP plasmas when the current profile is controlled. The electron flux reduction occurs over the entire plasma cross section. Density fluctuations are also reduced over the entire cross section, and are identified to be predominantly core-resonant tearing fluctuations. Future work seeks to better understand the means by which fluctuations are reduced by the application of auxiliary current drive and this understanding may allow further significant increases in electron particle and energy confinement.

The authors are especially grateful for the contributions of J. T. Chapman, D. Holly, J. S. Sarff, and the MST group. This work was supported by the U.S. Department of Energy.

[1] K. H. Burrell, Plasma Phys. Controlled Fusion **36**, A291 (1994).
[2] K. H. Burrell, Phys. Plasmas **4**, 1499 (1997).
[3] H. A. B. Bodin and A. A. Newton, Nucl. Fusion **19**, 1255 (1980).
[4] P. W. Terry and P. Diamond, Phys. Fluids B **2**, 428 (1990).
[5] M. R. Stoneking, S. A. Hokin, S. C. Prager, G. Fiksel, H. Ji, and D. J. Den Hartog, Phys. Rev. Lett. **73**, 549 (1994).
[6] G. Fiksel, S. C. Prager, W. Shen, and M. Stoneking, Phys. Rev. Lett. **72**, 1028 (1994).
[7] J. S. Sarff, N. E. Lanier, S. C. Prager, and M. R. Stoneking, Phys. Rev. Lett. **78**, 62 (1997).
[8] R. Bartiromo, V. Antoni, T Bolzonella, A. Buffa, L. Marrelli, P. Martin, E. Martines, S. Martini, and R. Pasqualotto, Phys. Plasmas **6**, 1830 (1999).
[9] R. N. Dexter, D. W. Kerst, T. W. Lovell, S. C. Prager, and J. C. Sprott, Fusion Technol. **19**, 131 (1991).
[10] S. R. Burns, W. A. Peebles, D. Holly, and T. Lovell, Rev. Sci. Instrum. **63**, 4993 (1992).
[11] Y. Jiang, N. E. Lanier, and D. L. Brower, Rev. Sci. Instrum. **70**, 703 (1999).
[12] J. S. Sarff, S. A. Hokin, H. Ji, S. C. Prager, and C. R. Sovinec, Phys. Rev. Lett. **72**, 3670 (1994).
[13] C. B. Forest *et al.,* Bull. Am. Phys. Soc. **42**, 20 (1997).
[14] M. G. Rusbridge and A. R. Jacobson, J. Appl. Phys. **56**, 757 (1984).
[15] S. Masamune, Phys. Fluids **31**, 1231 (1988).
[16] J. C. Ingraham, R. F. Ellis, J. N. Downing, C. P. Munson, P. G. Weber, and G. A. Wurden, Phys. Fluids B **2**, 143 (1990).
[17] P. G. Weber *et al.,* Plasma Phys. Controlled Nucl. Fusion Res. **2**, 509 (1990).
[18] G. A. Wurden *et al.,* Europhys. Conf. Abst. **12B**, 533 (1998).
[19] L. C. Johnson and E. Hinnov, J. Quant. Spectrosc. Radiat. Transfer **13**, 333 (1973).
[20] R. A. Hulse, Nucl. Technol./Fusion **3**, 259 (1983).
[21] T. D. Rempel, C. W. Spragins, S. C. Prager, S. Assadi, D. J. Den Hartog, and S. Hokin, Phys. Rev. Lett. **67**, 1438 (1991).
[22] S. Ortolani and D. D. Schnack, *Magnetohydrodynamics of Plasma Relaxation* (World Scientific, Singapore, 1993).
[23] A. F. Almagri, S. Assadi, S. C. Prager, J. S. Sarff, and D. W. Kerst, Phys. Fluids B **4**, 4080 (1992).
[24] J. S. Sarff, S. Assadi, A. F. Almagri, M. Cekic, D. J. Den Hartog, G. Fiksel, S. A Hokin, H. Ji, S. C. Prager, W. Shen, K. L. Sidikman, and M. R. Stoneking, in special issue on the *34th Annual Meeting of the Division of Plasma Physics of the American Physical Society,* Phys. Fluids B **5**, (1993).